11th International Conference on Advanced Materials
Rio de Janeiro Brazil
September 20 - 25

ICAM2009

Malleable Hypoeutectic Zr-Ni-Cu-Al Bulk Glassy Alloys with Tensile Plastic Elongation at Room Temperature

Yoshihiko Yokoyama(1)*, Kazutaka Fujita(2), Alain Reza Yavari(3) and Akihisa Inoue(1)

(1) IMR, Tohoku University, Katahira, Sendai 980-8577, Japan, e-mail: yy@imr.tohoku.ac.jp
(2) Department of Mechanical Engineering, Ube National College of Technology, Ube 755-8555, Japan
(3) SIMAP-CNRS, Institut Polytechnique de Grenoble, BP 75, Saint Martin□'Heres Campus, 38402 France
* Corresponding author.

Abstract – A new bulk glassy alloy (BGA) showing macroscopic tensile plastic elongation at room temperature has been developed in the hypoeutectic Zr-Ni-Cu-Al alloy system. The hypoeutectic Zr-Ni-Cu-Al BGA shows a high Poisson's ratio, a low Young's modulus and is highly malleable in compression. It exhibits a Poisson's ratio of 0.39, a Young's modulus of 73 GPa, and a distinct tensile plastic elongation of about 1.7 % at room temperature with necking due to the operation of many shear bands. The tensile plastic deformability seems to originate from modifications of the glass structure with increasing the number of Zr-Zr atomic pairs in the hypoeutectic composition.

Figure 1 (a) shows compositional dependence of Poisson's ratio of as-cast hypoeutectic Zr-Ni-Cu-Al_{10} glassy rods of diameter 8 mm. Near the eutectic composition of $Zr_{54}Ni_6Cu_{30}Al_{10}$, the Poisson's ratio decreases monotonically with increasing Cu content alone and increases with simultaneous rise in both Zr and Ni contents. $Zr_{70}Ni_{15}Cu_5Al_{10}$ BGA exhibits the highest Poisson's ratio among hypoeutectic alloys with ν = 0.38. Figure 1 (b) shows the compositional dependence of Young's modulus as well as Poisson's ratio. $Zr_{70}Ni_{15}Cu_5Al_{10}$ BGA also exhibits the lowest Young's modulus of E = 78 GPa. Since the compositional dependence of Young's modulus in Zr-Ni-Cu-Al BGA has a positive correlation with Al content, we modify the $Zr_{70}Ni_{15}Cu_5Al_{10}$ alloy composition, and we found the Zr-enriched hypoeutectic $Zr_{70}Ni_{16}Cu_6Al_8$ glassy alloy with the highest Poisson's ratio of 0.393±0.003 and the lowest Young's modulus of 73±4 GPa.

Figure 2 (a) shows the corresponding stress-strain curve. One can see a distinct linear elastic region, followed by clear yielding and then plastic elongation. Figure 2 (b-e) shows an over view of the tensile fracture surface of the $Zr_{70}Ni_{16}Cu_6Al_8$ BGA with a tensile true plastic strain of 1.7 %. Many shear band steps are observed on the surface near the wide sliding region (Fig. 2 (b)). Near the center of fracture surface, we can see the typical flower like vein patterns even in the tensile stress mode, as shown in Fig. 2 (c). Behind the fracture surface, shear band traces are seen on the outer surface, as shown in Fig. 2 (d), and the magnified image reveals the existence of many shear band steps near the fracture surface (Fig. 2 (e)) implying the formation of a single glassy phase.

The structures of bulk metallic glasses are characterized by the packing together of efficiently packed atom clusters (chemical and topological short range order (SRO) on a scale of about 0.5 nm) with the inter-cluster connectivity defining the medium range order (MRO) detectable to 1-2 nm in range by diffraction methods. This MRO is the same scale as the dimension of shear transformation zones (STZs) which must be stress-activated and is connected to initiate a shear band. The significant decrease in Young's and shear moduli in Zr-enriched BGAs (Fig.1 (b)) may be caused by the formation of bifurcated percolation path composed of weakly bonded regions enriched in nearest Zr-Zr atom pairs.

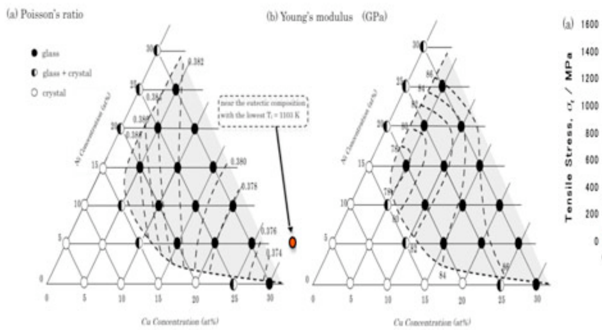

Figure 1: Compositional dependence of (a) Poisson's ratio and (b) Young's modulus of hypoeutectic Zr-Ni-Cu-Al_{10} BGAs.

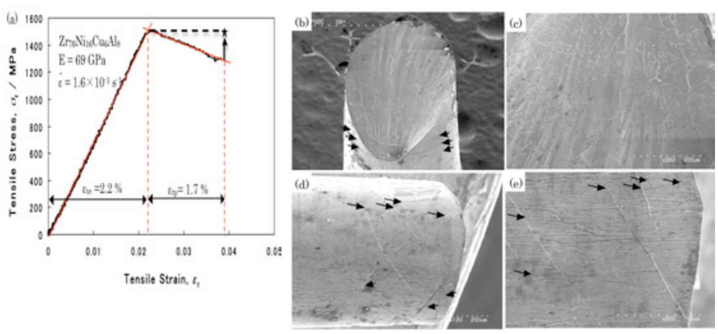

Figure 2: (a) Tensile stress-strain curve of hypoeutectic $Zr_{70}Ni_{16}Cu_6Al_8$ BGA; star mark corresponds to the estimated true stress just before fracture. (b) SEM images of over-all tensile fracture surface, (c) centre region of tensile fracture surface, (d) behind the tensile fracture surface and (e) magnified image of (d). Arrow marks point to surface steps created by shear bands near the tensile fracture surface.